

1 **PM_{2.5} Exposure Close to Marijuana Smoking and Vaping: a Case**
2 **Study in Residential Indoor and Outdoor Settings**

3 Kai-Chung Cheng,^{1*} Wayne Ott,¹ Lance Wallace², Yifang Zhu³, Lynn
4 Hildemann¹

5 ¹Stanford University, Stanford, CA; ²Retired, Santa Rosa, CA; ³University of California-Los
6 Angeles, Los Angeles, CA

7 *corresponding author: kccheng@stanford.edu

8

9 **ABSTRACT**

10 We conducted 35 experiments for spatial measurement of marijuana
11 aerosols in a current smoker's residential spaces. Fine particulate matter
12 (PM_{2.5}) concentrations were measured every second at 1, 2, and 3 m
13 horizontal distances from the smoker who performed prescribed 5-min
14 smoking and vaping activities. In each experiment, five SidePak monitors
15 measured PM_{2.5} concentrations at five different angles facing the front of the
16 smoker, representing the worst-case exposures. We studied the effect of
17 distance from the smoker for two marijuana sources - smoking a marijuana
18 cigarette, or *joint*, and vaping a liquid-cartridge vaping pen. Experiments
19 were conducted in the family room indoors and in the backyard outdoors
20 where the smoker normally consumes marijuana. Indoor marijuana vaping
21 had higher average exposures (5-min PM_{2.5}) at 1 m distance than indoor
22 marijuana smoking, but the levels from indoor vaping decreased more
23 rapidly with distance (e.g., 77% reduction for vaping versus 33% for smoking
24 from 1 to 2 m). Smoking and vaping in the outdoor environment reduce the

25 average exposures down to <5% of the indoor levels at each distance.
26 Cumulative frequency distributions of the 1-s PM_{2.5} concentrations revealed
27 the frequencies of exceeding any selected transient peak exposure limit at a
28 given distance. The frequency of exceedance decreased more quickly with
29 distance for vaping than for smoking. Smoking and vaping outdoors made
30 the transient peak exposures close to the source much less frequent than
31 smoking and vaping indoors (e.g., <1% exceeded 1000 µg/m³ outdoors
32 versus >20% indoors at 1 m). Plotting the frequency of exceedance versus
33 distance could offer additional guidance for a recommended minimum
34 distance from a marijuana source.

35

36 **INTRODUCTION**

37 The District of Columbia and 15 States – Alaska, Arizona, California,
38 Colorado, Illinois, Maine, Massachusetts, Michigan, Montana, Nevada, New
39 Jersey, Oregon, South Dakota, Vermont, and Washington have legalized
40 recreational marijuana use. As a result, involuntary exposure to secondhand
41 marijuana smoke has become much more common in everyday settings
42 across the country. Studies have shown that secondhand exposure close to
43 tobacco smoking or vaping is substantially higher than farther away (e.g.,
44 Acevedo-Bolton et al, 2014; Ott et al, 2014; Nguyen et al, 2019) – this
45 “*proximity effect*” will also be an issue near marijuana smoking or vaping.

46 The initial research investigating the proximity effect and spatial variation
47 of exposure near a source used a tracer gas to mimic the transport of

48 emitted air pollutants. For example, McBride et al (1999) released carbon
49 monoxide (CO) as a tracer in a residential living room while using 12 real-
50 time CO monitors to measure concentrations at different indoor positions.
51 Acevedo-Bolton et al (2012) deployed a larger monitoring array (30-37 CO
52 monitors) in the same residential living room to characterize exposure as a
53 function of the distance from a continuous CO source. Klepeis et al (2009)
54 measured real-time CO concentrations at up to 36 points in a residential
55 backyard to consider the proximity effect outdoors near a building. These
56 tracer gas studies provided insight into how different environmental
57 conditions (e.g., indoor ventilation or outdoor wind) influence the proximity
58 effect; however, they did not account for the characteristics of real smoking
59 or vaping emissions, such as the exhalation of mainstream smoke and the
60 buoyancy of sidestream smoke that can also affect proximity exposure
61 greatly.

62 Studies involving real human smoking or vaping were conducted mostly in
63 prescribed settings. Acevedo-Bolton et al (2014) performed controlled
64 experiments inside 2 homes (including a 158 m³ living room) and 16 outdoor
65 locations, using a small group of investigators wearing personal exposure
66 monitors to measure PM_{2.5} exposure close to prescribed tobacco cigarette
67 smoking. Ott et al (2014) used a similar small-group monitoring approach to
68 measure PM_{2.5} exposure near prescribed tobacco cigarette smoking at 6
69 outdoor bus stops on California roadways. Zhao et al (2017) measured
70 indoor PM_{2.5} concentrations at 4 different distances from volunteers

71 performing e-cigarette vaping, using a standardized puff frequency (every 30
72 s) indoors in an 80 m³ patient room in a clinical research center. Using a
73 heated mannequin, Martuzevicius et al (2019) measured indoor particle
74 exposures at 3 different distances from e-cigarette vaping, adopting the
75 same 30 s puff frequency. Nguyen et al (2019) investigated particle
76 concentrations at personal-space, social-space, public-space distances from
77 non-prescribed vaping activities in California vaping shops. These studies
78 provided valuable data for the levels of exposure close to tobacco smoking
79 or vaping in real-world indoor and outdoor settings.

80 Marijuana is most often smoked in homes (Berg et al, 2015; Berg et al,
81 2018). Using a commercial real-time sensor (Dylos™ DC1700 monitor), a
82 recent research study (Klepeis et al, 2017; Posis et al, 2019) monitored
83 particle number concentrations in ~300 California residences. This study
84 provided the first set of data on particle levels inside real homes with
85 marijuana smoking. However, this large-scale study did not allow spatial
86 measurement of exposure inside a home or accurate mass concentration
87 measurements based on gravimetric calibration. Little is known about the
88 PM_{2.5} exposure close to a marijuana smoker. There also is virtually no
89 knowledge of how different source types (smoking vs. vaping) and
90 environments (indoor vs. outdoor) affect the proximity effect.

91 Our first goal was to examine, for the first time, PM_{2.5} exposure close to a
92 marijuana smoker and how the exposure can be reduced by increasing the
93 distance from the source; we measured real-time PM_{2.5} concentrations at 1,

94 2, and 3 m distances from marijuana emissions in a smoker's home and
95 assessed both the level and frequency of exposure versus distance. Our
96 second goal was to investigate whether choosing a different source type, a
97 different location, or a different environmental setting can reduce the
98 proximity exposure; we tested two common marijuana source types (the
99 joint and the vaping pen) along with their corresponding exhalation patterns
100 in an indoor and an outdoor location under different ventilation and air
101 mixing conditions. Given the collected exposure data, an additional goal of
102 our research was to explore data analysis methods that can potentially be
103 useful for evaluating the recommended physical distance from marijuana
104 sources to minimize involuntary exposure.

105

106 **METHODOLOGY**

107 **Participant.** A habitual user of marijuana (a 40-50 year old male) was
108 recruited in this study. The cannabis materials were provided by the
109 participant and consumed in his regular smoking spaces. The study protocol
110 was accepted by the participant and approved by the Institutional Review
111 Board at Stanford University.

112 **Experimental Setup.** We performed field research inside a residential
113 property in San Jose, CA (Figure 1). This single-family home has two stories
114 and a private backyard, and the marijuana smoker is the only occupant in
115 this property. Five AM510 SidePak™ monitors (TSI, Shoreview, MN, USA)
116 were deployed near the *indoor chair* in the 4.3×3.7×2.4 m (38 m³) family

117 room or the *outdoor chair* in the backyard where the participant normally
118 smokes or vapes marijuana (see the chairs marked with stars in Figure 1).
119 Both chairs backed up to a wall, and the outdoor chair had a small table 0.7
120 m high to its immediate left. The 5 SidePak monitors were placed radially
121 with 15° angle spacing at an equal distance from the source in each session
122 (1 m, 2m, or 3m), measuring PM_{2.5} concentration every 1 s; they were facing
123 the front of the smoker to account for the worst-case exposure. Three
124 monitors were placed at 1 m height (black circles), whereas two monitors
125 were at 1.5 m height (white circles) to consider typical adult breathing
126 heights while sitting and standing, respectively (Figure 1). The actual
127 measured breathing heights of the smoker sitting on the indoor and outdoor
128 chairs were 1.2 m and 1.1 m, respectively.

129 Using these monitoring settings, we performed 35 experiments (20 indoors
130 and 15 outdoors). For the indoor experiments, 17 were performed with all
131 windows and interior or exterior doors closed in the house - “base case”
132 while 3 involved opening the family-room door (18” open) and two dining
133 room windows (each 15” open) while running the fan of the centralized HVAC
134 system (with one ceiling register in each room) - “alternative case”. For
135 outdoor experiments, 12 were carried out with a fully-opened outdoor
136 umbrella above the smoker (2 m height and 1.9 m in diameter) - “base case”
137 - while 3 were carried out with this umbrella fully closed (<0.1 m in
138 diameter) - “alternative case”. We hypothesize opening or closing the
139 umbrella would noticeably affect the air mixing and proximity effect close to

140 the source. For the base-case experiments, all 5 monitors were underneath
141 the umbrella when placed at 1 m distance from the smoker.

142 **Air Velocity and Ventilation.** We used the VelociCalc 8386
143 anemometer (TSI, Shoreview, MN, USA) to measure and log the indoor and
144 outdoor air velocities near the smoking or vaping locations every 2 s during
145 each experiment. This instrument has a 6-mm diameter sensor probe with a
146 25 mm long anemometer at its tip, and its minimum detectable air speed is
147 0.01 m/s. It was not possible to release carbon monoxide or sulfur
148 hexafluoride tracer gas in the participant's house. As a way to estimate the
149 magnitude of ventilation, we burned matches inside the house while using
150 the Optical Particle Sizer 3330 (TSI, Shoreview, MN, USA) to measure the
151 particle number concentrations every 1 min. The air change rate (ACH) was
152 estimated by the log linear regression between concentration of the smallest
153 particle size range (0.3-0.374 μm) and time after the well-mixed condition
154 was reasonably achieved. Given the timescale of the experiments (1-2 h),
155 diffusional and gravitational losses of particles within this size range were
156 expected to be negligible compared with air exchange; this method has been
157 used to estimate ACH in a residence where tracer gas releases were not
158 feasible (e.g., Cheng et al 2020). These air change rate tests were performed
159 outside the regular smoking or vaping experiments, because they involved
160 particle emissions.

161 **Sources and Protocol.** We investigated two types of marijuana sources
162 regularly used by the participant: (i) a cigarette-like marijuana joint (Caliva

163 “Toasties”) with 0% CBD and 9.6% THC, and (ii) an electronic vaping pen
164 (AbsoluteXtracts, ABX) with the “Care by Design” 2:1 cartridge (CBD 46.1%
165 and THC 21.9%). A standardized smoking or vaping protocol that consisted
166 of 5 puffs over a 5-minute period was used. After inhaling, the participant
167 exhaled at the starting point of every minute (black areas in Figure S1); we
168 defined the 5 min period as the source period. This protocol was intended to
169 enable comparisons between experiments with different source types or
170 source distances based on the same exhalation or emission frequency (once
171 every minute). Zhao et al (2017) and Martuzevicius et al (2019) have
172 adopted this approach but with a different frequency (once every 30 s) for e-
173 cigarette vaping. In our study, the participant chose the 1-min time interval
174 for the 5-puff sequence to not exceed his normal habit of smoking and
175 vaping. We did not choose a specific volume and duration for each puff,
176 since we wanted to preserve the behavioral differences embedded in each
177 puff for different source types (smoking versus vaping) and to investigate
178 how they may affect the spatial variation of exposure close to a source.

179 The participant did not permit sensors to be used in contact with his body;
180 therefore, puff topography or spirometry measurement involving sensor
181 mouthpiece breathing was not conducted in this study. As a surrogate
182 approach, we placed the VelociCalc anemometer in front of the smoker
183 during the 5-min source period (Figure S1) at 0.1 m horizontal distance from
184 the mouth position to record the “exhalation peak velocity” – the maximum
185 air velocity produced by each exhalation (see Figure S2). This approach

186 enabled us to investigate human exhalation via air environment
187 measurement. We discovered the temporal fluctuations of air velocities
188 outdoors were comparable to the magnitudes of exhalation peak velocities.
189 Therefore, we were not able to measure the exhalation peak velocities in the
190 outdoor experiments. The durations of the exhalation were measured by the
191 participant using a stopwatch. A test examining how consistently exhalation
192 peak velocities can be produced and measured by the environmental
193 sensing method is available in the Supplementary Material (Figure S3).

194 **PM_{2.5} Calibration.** To ensure consistent measurements between
195 monitors, we conducted a separate quality assurance study in which we
196 placed 17 SidePak monitors (including the 5 monitors used in this study)
197 inside a car chamber (2006 Honda Element) with a smoke source,
198 simultaneously measuring PM_{2.5} concentrations every 1 min. After the
199 emission stopped and well-mixed condition was reasonably achieved
200 (*gamma period*, Ott, 2007), the exponentially decaying measurements of the
201 SidePak monitors were compared by linear regression with our reference
202 SidePak monitor, giving $R^2 > 0.999$ for the 5 SidePak monitors used (forcing
203 zero intercept). The slope of each linear regression (0.87-1.03) was used to
204 rescale each measuring device to agree with the reference monitor.

205 The SidePak monitors measure PM_{2.5} concentration based on light
206 scattering properties, which are affected by the particle size and
207 composition. To accurately represent the actual PM_{2.5} concentration, the
208 calibration factor (CF) - the ratio of gravimetrically-to-optically-measured

209 PM_{2.5} concentration is needed for each source type (e.g., Jiang et al, 2011;
210 Dacunto et al, 2013). In a previously published paper, we determined the
211 CFs for the two marijuana source types: 0.35 for joint smoking and 0.44 for
212 vaping (Zhao et al, 2020) for the reference SidePak monitor; they were
213 applied along with the inter-monitor slopes to rescale all PM_{2.5} measurement
214 in this study (e.g., actual concentration for vaping = direct reading of
215 SidePak_{*i*} × (0.44/[slope of SidePak]_{*i*}) where *i* = 1-5). Jiang et al (2011) found
216 that CFs for SidePak monitors remained relatively constant over time; for a
217 16-month period, the average difference was ~3%. The particle zero filter
218 was attached to the inlet of each SidePak monitor immediately before each
219 experiment for zero calibration.

220 **Decay and Mixing Characterization.** The PM_{2.5} measurements at the 3
221 different distances (1 m, 2 m, and 3 m) were collected from separate
222 experiments, not simultaneously. It is important to ensure comparisons were
223 made based on comparable environmental settings. In each experiment,
224 therefore, we included a 5-min sampling period prior to the source period to
225 account for the variation in PM_{2.5} background concentration. For each indoor
226 experiment, we added a 60-min sampling period following the source period
227 for determining the PM_{2.5} decay inside the building. The decay rates were
228 determined by the log linear regressions between 1-min PM_{2.5} concentrations
229 averaged over the 5 monitors (background subtracted) versus time during
230 the well-mixed decay periods. For the same source type (with the same
231 aerosol volatility), the PM_{2.5} decay rate (the sum of the air change rate,

232 surface deposition rate, and evaporation loss rate) could reflect the relative
233 strength of air mixing indoors. A higher air change rate will lead to stronger
234 indoor air mixing (Drivas et al, 1996; Cheng et al, 2011), enhancing the
235 particle surface deposition (e.g., Thatcher et al, 2002; He et al, 2005; Xiao et
236 al, 2020). This suggests both the cause and consequence of stronger air
237 mixing could contribute to a higher decay rate. Therefore, given a
238 comparable evaporation loss rate (the same source type), a larger decay
239 rate could indicate stronger air mixing indoors, which could cause more
240 uniform concentration and a smaller proximity effect. Air mixing is one
241 governing factor that affects the spatial distribution of concentration and
242 exposure close to a source (e.g., Drescher et al, 1995; Cheng et al, 2011;
243 Cheng et al, 2020). By examining the decay rates for experiments with the
244 same source type, we can ensure comparisons are based on comparable air
245 exchange and air mixing conditions.

246

247 **RESULTS AND DISCUSSION**

248 To determine the source and environmental characteristics in each indoor
249 experiment, we calculated the average exhalation peak velocity and duration
250 (averaged over 5 puffs) and the decay rate (from log-linear regression).
251 Table 1 summarizes the statistics of average exhalation peak velocities,
252 average exhalation durations, and decay rates for indoor smoking versus
253 indoor vaping from 16-17 experiments with all the windows and doors closed
254 without fan operating ($ACH = 0.31-0.34 \text{ h}^{-1}$). These base-case experiments

255 had background air velocities below the anemometer's detection limit (<0.01
256 m/s) - this enabled more accurate determination of exhalation velocities for
257 the two different sources. The mean of average exhalation peak velocities
258 for indoor smoking (0.99 m/s) was ~ 2 times as high as that for indoor vaping
259 (0.53 m/s). The mean of average exhalation durations for indoor smoking
260 (2.3 s) was $\sim 70\%$ of that for indoor vaping (3.4 s). The mean decay rate for
261 indoor vaping was higher than the mean decay rate for indoor smoking (0.75
262 versus 0.46 h^{-1}). Particle losses due to air exchange and particle settling are
263 expected to be comparable for indoor smoking and vaping experiments; the
264 sizable difference was likely due to the higher aerosol volatility for vaping.
265 This finding was consistent with previous studies testing the decay rates of 4
266 different marijuana sources (joint, glass pipe, water pipe, and vaping pen)
267 inside a car chamber (Zhao et al, 2020) and in a residential bedroom (Ott et
268 al, 2020). Li et al (2020) found $\text{PM}_{2.5}$ particle loss rates for vaping aerosols
269 (from e-cigarettes in this case) were >4 times as high as that for - Di-Ethyl-
270 Hexyl-Sebacat (DEHS) aerosols with little evaporation. In addition to
271 exhalation pattern, aerosol evaporation could have a significant effect on
272 exposure versus distance from the source.

273 The average air velocities for outdoor experiments ranged from 0.21 to
274 0.33 m/s. The highest average velocity (0.33 m/s) was recorded when the
275 overhead outdoor umbrella was folded (alternative case). This could be due
276 in part to less blockage of the air movement. Klepeis et al (2009) and
277 Acevedo-Bolton et al (2014) measured ground-level air velocities in the

278 backyard of a California home. Their reported average air velocities (0.26-
279 0.34 m/s) were comparable to our measured values. These backyard
280 measurements are expected to be affected by eddy currents near buildings.

281 Figures 2(a) and 2(b) show examples of the 1-s concentration time series
282 of PM_{2.5} measured indoors (top) and outdoors (bottom) at 1 m, 2 m, and 3 m
283 horizontal distances from the participant performing marijuana vaping in the
284 residential property (Figure 1). Unlike the standard indoor experiments that
285 were performed separately with 1-h decay periods (see the Decay and
286 Mixing Characterization section), continuous indoor measurements were
287 taken across multiple source periods (grey areas) with only 5 minutes apart.
288 This was to align with the emission sequence of the outdoor time series to
289 allow comparisons between Figures 2(a) and 2(b). Here, all concentrations
290 greater than the monitor's upper limit were replaced with 20 mg/m³ (CF = 1),
291 giving maximum concentrations ~10 mg/m³ (CF = 0.44).

292 For both the indoor and outdoor experiments, the magnitudes and
293 occurrences of transient concentration spikes - "*microplumes*" (e.g.,
294 Acevedo-Bolton et al, 2012; Cheng et al, 2014) - increased with decreasing
295 distances, showing the proximity effect during active emissions (light grey
296 regions in Figure 2). Striking differences were observed between indoor and
297 outdoor situations. Microplumes were much more likely indoors than
298 outdoors. In the indoor environment (without mechanical ventilation),
299 aerosols could follow the exhaled airflow, moving toward the monitors that
300 were in front of the vaper. In contrast, aerosol movement outdoors was

301 primarily governed by the wind patterns. The rapidly changing directionality
302 of outdoor airflows near the building made microplumes less likely to
303 emerge. The durations of microplumes were longer indoors than outdoors.
304 The slower air movement indoors could make emitted plumes linger at a
305 monitoring location. This effect can also be seen from the persistent PM_{2.5}
306 concentration time series after each source emission period ended indoors.
307 As expected, the more frequent occurrences and longer durations of
308 microplumes indoors greatly increased the average concentration and
309 exposure at close proximity to the active emission source.

310 Figure 3 summarizes the time-averaged PM_{2.5} concentrations over the 5-
311 min source periods at 1, 2, and 3 m distances from the source in all the 35
312 indoor and outdoor experiments with marijuana smoking and vaping.
313 Figures 3(a)-3(b) correspond to the condition with all windows and doors
314 closed and without HVAC fan running (indoor base case) whereas Figure 3(c)
315 involves opening a door and two windows and with HVAC fan running (indoor
316 alternative case). Figures 3(d)-3(e) correspond to the condition with the
317 umbrella open and above the smoker (outdoor base case) whereas Figure
318 3(f) involves fully closing the overhead umbrella (outdoor alternative case).
319 Each boxplot contains measurements from the 5 SidePak monitors at
320 different angles in front of the smoker (Figure 1) with the dashed line
321 representing the mean value and the solid line representing the median.
322 Background concentrations ranged from 1.2 to 6.8 $\mu\text{g}/\text{m}^3$; they were

323 subtracted from these 5-min PM_{2.5} averages. Statistics of each boxplot are
324 available in the Supplementary Material (Table S1).

325 The 5-min PM_{2.5} concentrations at 1 m were higher and more variable for
326 indoor vaping than for indoor smoking (mean = 1330 versus 870 $\mu\text{g}/\text{m}^3$;
327 interquartile range = 1260 versus 670 $\mu\text{g}/\text{m}^3$; Figure 3(b) versus 3(a)).
328 However, the levels of indoor vaping decreased more noticeably with
329 distance than for indoor smoking (77% versus 33% reduction from 1 to 2 m
330 and 63% versus 50% reduction from 2 to 3 m). This finding could be
331 associated with the difference in exhalation pattern - the exhalation peak
332 velocity for indoor vaping was only ~50% that of indoor smoking. Therefore,
333 vaping aerosols are expected to have longer time for decay before reaching
334 a given distance. Another consideration involves the aerosol evaporation
335 process - the higher decay rate (>1.6 times higher) of the vaping aerosols
336 due to their higher volatility could also result in a greater concentration
337 decrease over distance.

338 The PM_{2.5} exposures for indoor marijuana smoking (870 $\mu\text{g}/\text{m}^3$ at 1 m and
339 580 $\mu\text{g}/\text{m}^3$ at 2 m; Figure 3(a)) were much higher than for indoor tobacco
340 smoking (320 $\mu\text{g}/\text{m}^3$ at 1.25 m and 60 $\mu\text{g}/\text{m}^3$ at 2 m; Acevedo-Bolton et al,
341 2014). This could be caused by the higher emission rate for marijuana
342 smoking (7.8 mg/min versus 2.2 mg/min; Ott et al, 2020) accompanied with
343 the smaller indoor volume (38 versus 158 m^3). Another factor was the
344 different monitoring setups - our study used 5 monitors to cover 60° angle
345 facing the smoker, making it more likely to capture the emitted plumes than

346 a single monitor. Similarly, $PM_{2.5}$ exposures for indoor marijuana vaping
347 ($1330 \mu\text{g}/\text{m}^3$ at 1 m and $310 \mu\text{g}/\text{m}^3$ at 2 m; Figure 3(b)) were much higher
348 than indoor e-cigarette vaping ($375 \mu\text{g}/\text{m}^3$ at 0.8 m and $7 \mu\text{g}/\text{m}^3$ at 2 m; Zhao
349 et al, 2017). This again was likely due to more monitors at each distance (5
350 versus 1) and the smaller indoor volume (38 versus 80 m^3). Both vaping
351 sources had a significant concentration decrease over distance, but the
352 marijuana decrease was smaller (77% versus 98%). This could be due in
353 part to the lower aerosol volatility of marijuana vaping compared to e-
354 cigarette vaping (Wallace et al, 2021).

355 Figure 3(c) shows the measurements from the only 3 indoor vaping
356 experiments (one for each distance) with the HVAC fan operating in the
357 house (alternative case). In addition to lowering the 5-min $PM_{2.5}$ levels (due
358 to increased aerosol removal), mechanical ventilation greatly reduced the
359 variation of the 5-min $PM_{2.5}$ averages measured at the 5 different angles at
360 each distance (Figure 3(c) versus 3(b)). In addition, it diminished the
361 pronounced concentration gradient over distance observed without
362 mechanical ventilation operating. As expected, stronger air mixing due to
363 mechanical ventilation made the $PM_{2.5}$ concentration more uniform in space.

364 The outdoor 5-min $PM_{2.5}$ levels at each distance were less than 5% of the
365 indoor levels for either smoking or vaping. Therefore, a different vertical
366 (concentration) scale was needed for Figures 3(d)-3(f). Again, the varied
367 airflow direction and more rapid plume movement outdoors made the $PM_{2.5}$
368 exposures in front of the smoker much lower than indoors. The $PM_{2.5}$

369 exposure for outdoor marijuana smoking (mean = 43 $\mu\text{g}/\text{m}^3$ at 1 m; Figure
370 3(d)) was higher than for outdoor tobacco smoking: 13 $\mu\text{g}/\text{m}^3$ at 1 m (Klepeis
371 et al, 2007) and 29 $\mu\text{g}/\text{m}^3$ at 0.8-1.5 m (Acevedo-Bolton et al, 2014). In
372 addition to the higher emission rate for marijuana smoking (Ott et al, 2020),
373 use of 5 1-m monitors under an outdoor umbrella with the smoker made
374 plume encounters more likely (see Figure 1). Most of the outdoor
375 experiments involved the participant smoking or vaping under an outdoor
376 umbrella (base case) except for the 3 alternative-case experiments in Figure
377 3(f) (one for each distance with 5 SidePak monitors). In these 3 experiments
378 without an umbrella above the smoker, the lower exposures were likely
379 caused by the less-enclosed setting. This, in combination with the highest
380 recorded average air velocity (0.33 m/s), could cause greater dispersion of
381 emitted particles near the smoker.

382 For each box plot in the 4 base-case graphs (Figures 3(a)-3(b) and Figures
383 3(d)-3(e)), we separated the 5-min averages into two groups based on 1 and
384 1.5 m breathing heights and calculated the mean for each group. For indoor
385 vaping, the means of the 5-min averages for all the 3 distances (1 m, 2 m,
386 and 3 m) were higher at 1 m than at 1.5 m height (Figure S4(b)). This is not
387 surprising as the source was closer to 1 m height. In contrast, the means for
388 all the 3 distances were higher at 1.5 m than at 1 m height for indoor
389 smoking (Figure S4(a)). The difference was greatest at the shortest distance
390 (1 m); the mean at 1.5 m height was ~ 1.7 times as high as the mean at 1 m
391 height. This might be due to the stronger plume buoyancy created by a

392 combustion source - the burning joint - thus increasing the means at 1.5 m
393 height. The means of the 5-min averages outdoors (Figures S4(c)-4(d)) did
394 not necessarily follow the same pattern observed indoors; for outdoor
395 smoking (Figure S4(c)), the mean at the 1.5 m height was greater at 1 m
396 distance, but the outdoor means at 1 m height became greater at the 2 and
397 3 m distances. In the presence of outdoor wind, the effect of plume
398 buoyancy could become less noticeable, especially for greater distances
399 from the source.

400 Figures 4(a)-4(f) show the cumulative frequency distributions of 1-s $PM_{2.5}$
401 concentrations collected during 5-min source periods on log-probability
402 graphs for 18 indoor and outdoor experiments with smoking and vaping.
403 Again, the left four graphs corresponded to the base-case experiments
404 indoors (Figures 4(a)-4(b); with all windows and doors closed; without HVAC
405 fan running) and outdoors (Figures 4(d)-4(e)); outdoor umbrella open above
406 the smoker). The right two graphs (Figures 4(c) and 4(f)) corresponded to
407 the alternative-case experiments indoors (opening a door and two windows
408 and running the HVAC fan) and outdoors (folding the overhead umbrella),
409 respectively. Each frequency distribution contains aggregated
410 measurements from the 5 SidePak monitors at different angles ($n = 1500$).
411 Each graph compared the cumulative frequency distributions at 1, 2, and 3
412 m distances from the 3 experiments with similar environmental conditions.
413 Indoor experiments that had comparable decay rates were grouped together
414 for each graph: $0.34-0.37 \text{ h}^{-1}$ for smoking (Figure 4(a)), $0.97-1.06 \text{ h}^{-1}$ for

415 vaping (Figure 4(b)), and 6.9-7.8 h⁻¹ for vaping with a door and two windows
416 opened and HVAC fan running (Figure 4(c)) (see Methodology section for
417 details). Experiments in each outdoor graph (Figures 4(d)-4(f)) were
418 conducted consecutively with 5 min intervals to minimize the outdoor
419 weather variation (e.g., Figure 2(b)). To avoid negative values for the log
420 scale concentrations, the background concentrations (2-6.8 μg/m³ indoors
421 and 3.3-3.9 μg/m³ outdoors) were included in these 1-s PM_{2.5} concentration
422 frequency distributions.

423 Plotting a cumulative frequency distribution on the log-probability graph,
424 one can visualize the frequency of exceeding any given concentration limit.
425 Taking figure 4(b) as an example, 10% of the concentrations exceeded 1000
426 μg/m³ at 2 m from the source. The frequency increased to ~40% at 1 m and
427 decreased to 0% at 3 m. For the same frequency of exceedance (10%), the
428 concentration limit increased to ~4000 μg/m³ at 1 m and decreased to ~150
429 μg/m³ at 3 m.

430 Compared to indoor smoking (Figure 4(a)), the frequency distributions for
431 indoor vaping (Figure 4(b)) showed much greater separation at the 3
432 distances. For example, from 1 to 3 m distance, the frequency of exceeding
433 1000 μg/m³ dropped ~40% (from 38 to 0%) for indoor vaping but only ~10%
434 (from 22 to 14%) for indoor smoking. The more noticeable decrease in the
435 frequencies for vaping again could be associated with the longer travel time
436 (due to lower breath exhalation peak velocity) and the higher decay rate
437 compared to smoking. Turning on the mechanical ventilation system (Figure

438 4(c)) flattened the cumulative frequency distribution at each distance for the
439 middle range of concentrations (50-500 $\mu\text{g}/\text{m}^3$). It also reduced the
440 separation of the 3 frequency distributions. In addition to the average
441 concentrations (5-min $\text{PM}_{2.5}$ in Figure 3(c)), the stronger mechanical air
442 mixing made the transient concentrations (1-s $\text{PM}_{2.5}$) become more uniformly
443 distributed in space.

444 Concentration peaks at each distance become much less likely to occur in
445 the outdoor settings than indoors. For example, for both smoking (Figure
446 4(d)) and vaping (Figure 4(e)), less than 1% exceeded 1000 $\mu\text{g}/\text{m}^3$ at the 1 m
447 distance outdoors compared to more than 20% indoors. At 2 and 3 m
448 distances, 0% of the 1-second concentrations exceeded 1000 $\mu\text{g}/\text{m}^3$ outdoors
449 while up to nearly 15% exceeded this level indoors. The separation of the
450 frequency distributions at different distances occurs at a higher cumulative
451 frequency range outdoors (50-70%; Figures 4(d)-4(e)) than indoors (5-10%;
452 Figures 4(a)-4(b)). Folding the overhead outdoor umbrella reduced the peak
453 concentrations at each distance; it also reduced the separation of the 3
454 cumulative frequency distributions (Figure 4(f) versus 4(e)). Like the indoor
455 case (Figure 4(c) versus 4(b)), this could be caused by the stronger air
456 mixing near the source due to a less enclosed environment, making the 1-s
457 $\text{PM}_{2.5}$ concentrations more uniform in space. In this case, all the measured 1-
458 s $\text{PM}_{2.5}$ concentrations dropped below 1000 $\mu\text{g}/\text{m}^3$ (0% frequency to exceed
459 1000 $\mu\text{g}/\text{m}^3$ for distances ≥ 1 m).

460 By obtaining cumulative frequency distributions of short-term
461 concentrations at multiple distances, one can create a graph that shows how
462 the frequency of exceedance varies with distance for a selected peak
463 exposure limit. For example, using the 3 cumulative frequency distributions
464 for outdoor smoking (Figure 4(d)), Figure (5) plotted frequency of
465 exceedance versus distance for 3 selected peak exposure limits (50, 100,
466 and 500 $\mu\text{g}/\text{m}^3$). A higher peak exposure limit (a less stringent limit) gave a
467 lower frequency of exceedance at each distance. For each peak exposure
468 limit, the frequency of exceedance decreased with increasing distance from
469 the source. The decreases were more significant for a lower peak exposure
470 limit (e.g., 50 $\mu\text{g}/\text{m}^3$), allowing the curves for the 3 limits to converge
471 gradually. Assuming the case where <1% of exceedance is needed, keeping
472 1 m distance from the source could not meet any of the 3 peak exposure
473 limits. Moving from 1 to 2 m distance, we could satisfy the least stringent
474 peak exposure limit (500 $\mu\text{g}/\text{m}^3$). All the 3 peak exposure limits can be met if
475 we moved further to the 3 m distance. The 24-h $\text{PM}_{2.5}$ standard offers a
476 benchmark for assessment of long-term average exposures. The data
477 analysis demonstrated here (Figures (4) and (5)) provides a possible
478 standardized method to evaluate transient exposures to marijuana aerosols.

479 **Limitations and Future Work.** Optical sensor measurement could drift
480 over time; it is optimal to calibrate optical monitors with the gravimetric
481 shortly before the field experiments. Smoking and exhalation patterns vary
482 across individuals; they could influence the concentration and spatial spread

483 of an emitted plume. For example, Fuoco et al (2014) and Zhao et al (2016)
484 found particle concentration of e-cigarette vaping increased with puff
485 duration; a higher exhalation velocity could increase the distance impacted
486 by the emission. Future experiments examining how these behavioral
487 patterns affect the proximity effect would be valuable. Particle size
488 distribution influences the deposition of inhaled aerosols. Future research
489 investigating the effect of distance on particle size distribution indoors and
490 outdoors would be useful. This study shows how high PM_{2.5} levels could be
491 inside a home with a marijuana smoker. PM_{2.5} has been associated with
492 cardiorespiratory diseases; marijuana-related PM_{2.5} also has the potential to
493 cause mental disorders. It is critical to examine the health effects of
494 marijuana secondhand exposure for household members at home (e.g.,
495 children who live with marijuana smokers).

496 **CONCLUSIONS**

497 In summary, a clear proximity effect was observed for both smoking
498 and vaping marijuana indoors without mechanical air mixing (HVAC fan
499 running). A proximity effect was also evident outdoors when the participant
500 smoked or vaped under a garden umbrella that limited air mixing. PM_{2.5}
501 exposures decreased more rapidly with distance from the source for vaping
502 than for smoking, mostly likely caused by higher volatility of vaping aerosols.
503 This finding suggests a smaller surrounding area of impact for vaping than
504 for smoking. Smoking and vaping outdoors will reduce both average and
505 transient peak exposures to exhaled aerosols. This is consistent with the

506 expectation that exposure to respiratory aerosols from a human source is
507 less likely outdoors than indoors in light of the current COVID-19 pandemic.
508 Previous measurements in Klepeis et al (2007) suggest outdoor exposure to
509 tobacco smoke can be reduced noticeably when a person is ≥ 2 m away from
510 the smoker. This is consistent with the results for outdoor marijuana smoking
511 and vaping in this case study. With the legalization of recreational marijuana,
512 cannabis smoking and vaping are rapidly emerging in everyday living
513 environments. There is a critical need to address the question regarding the
514 safe distance for marijuana smoking and vaping (e.g., can we apply the 12 ft
515 safe distance for tobacco smoking to marijuana smoking?). This study was
516 the first research systematically examining $PM_{2.5}$ exposure close to marijuana
517 smoking and vaping in indoor and outdoor environment. The determination
518 of the “concentration proximity curve” - average exposure versus the
519 distance from the source could inform the safe distance policy or advisory.
520 The characterization of the “frequency proximity curve” - frequency of peak
521 exposure exceedance versus distance proposed here could provide
522 additional insight into the related decision making. Results from a single
523 marijuana smoker in a few indoor and outdoor locations cannot represent all
524 possible exposure situations. Nonetheless, the initial proximity exposure
525 measurements, findings, and data analysis methods presented here would
526 be useful for the design of future field research investigating the proximity
527 effect and safe distance for marijuana smoking and vaping.

528

529 **ACKNOWLEDGEMENT**

530 This research was supported by a grant (Award# 28IR-0062) from the
531 Tobacco-Related Disease Research Program (TRDRP, Oakland, CA).

532

533 **REFERENCES**

534 Acevedo-Bolton, V., Cheng, K.C., Jiang, R.T., Ott, W.R., Klepeis N.E.,
535 Hildemann L.M., 2012. Measurement of the proximity effect for indoor air
536 pollutant sources in two homes. *Journal of Environmental Monitoring*, 14, 94-
537 104.

538

539 Acevedo-Bolton, V., Ott, W.R., Cheng, K.C., Jiang, R.T., Klepeis N.E.,
540 Hildemann L.M., 2014. Controlled experiments measuring personal exposure
541 to PM2.5 in close proximity to cigarette smoking. *Indoor Air*, 24, 199-212.

542

543 Berg, C.J., Buller, D.B., Schauer, G.L., Windle, M., Stratton, E., Kegler, M.C.,
544 2015. Rules regarding marijuana and its use in personal residences: findings
545 from marijuana users and nonusers recruited through social media, *Journal of*
546 *Environmental and Public Health* ID 476017.

547 <http://dx.doi.org/10.1155/2015/476017>. Accessed on January 19, 2021.

548

549 Berg, C.J., Haardörfer, R., Wagener, T.L., Kegler, M.C., Windle, M., 2018.
550 Correlates of allowing tobacco product or marijuana use in the homes of

551 young adults, *Pediatrics* 2018;141:S10. [https://doi: 10.1542/peds.2017-](https://doi.org/10.1542/peds.2017-1026E)
552 1026E. Accessed on January 9, 2021.

553

554 Cheng, K.C., Acevedo-Bolton, V., Jiang, R.T., Klepeis, N.E., Ott, W.R., Fringer,
555 O.B., and Hildemann, L.M., 2011. Modeling exposure close to air pollution
556 sources in naturally ventilated residences: Association of turbulent diffusion
557 coefficient with air change rate. *Environmental Science and Technology*, 45,
558 4016-4022.

559

560 Cheng, K.C., Acevedo-Bolton, V., Jiang, R.T., Klepeis, N.E., Ott, W.R., Kitanidis,
561 P.K., Hildemann, L.M., 2014. Stochastic modeling of short-term exposure
562 close to an air pollution source in a naturally ventilated room: An
563 autocorrelated random walk method. *Journal of Exposure Science and*
564 *Environmental Epidemiology*, 24, 311-318.

565

566 Cheng, K.C., Zheng, D., Hildemann, L.M., 2020. Impact of fan mixing on air
567 pollutant exposure near indoor sources: an analytical model to connect
568 proximity effect with energy. *Building and Environment*, 183, 107185.
569 <https://doi.org/10.1016/j.buildenv.2020.107185> Accessed on January 27,
570 2021.

571

572 Dacunto, P.J., Cheng, K.C., Acevedo-Bolton, V., Jiang, R.T., Klepeis, N.E.,
573 Repace, J.L., Ott, W.R., Hildemann, L.M., 2013. Real-time particle monitor

574 calibration factors and PM2.5 emission factors for multiple indoor sources.
575 *Environmental Science Processes & Impacts*, 15, 1511-1519.
576

577 Drescher, A.C., Losbascio, C., Gadgil, A.J., Nazaroff, W.W., 1995. Mixing of a
578 point-source indoor pollutant by forced convection. *Indoor Air*, 5, 204-214.
579

580 Drivas, P.J., Valberg, P.A., Murphy, B.L., Wilson, R., 1996. Modeling indoor air
581 exposure from short-term point source releases. *Indoor Air*, 6, 271-277.
582

583 Fuoco, F.C., Buonanno, G., Stabile, L., Vigo, P., 2014. Influential parameters
584 on particle concentration and size distribution in the mainstream of e-
585 cigarettes. *Environmental Pollution*, 184, 523-529.
586

587 He, C., Morawska, L., Gilbert, D., 2005. Particle deposition rates in residential
588 houses. *Atmospheric Environment*, 39, 3891-3899.
589

590 Jiang, R.T., Acevedo-Bolton, V., Cheng, K.C., Klepeis N.E., Ott, W.R., and
591 Hildemann L.M., 2011. Determination of response of real-time SidePak
592 AM510 monitor to secondhand smoke, other common indoor aerosols, and
593 outdoor aerosol. *Journal of Environmental Monitoring*, 13, 1695-1702.
594

595 Klepeis, N.E., Bellettiere, J., Hughes, S.C., Nguyen, B., Beradi, V., Liles, S.,
596 Obayashi, S., Hofstetter, C.R., Blumberg, E., Hovell, M.F., 2017. Fine particles

597 in homes of predominantly low income families with children and smokers:
598 Key physical and behavioral determinants to inform indoor-air-quality
599 interventions, *PLoS ONE* 12(5).e017718.
600 <https://doi.org/10.1371/journal.pone.0177718> Accessed on January 19, 2021.
601
602 Klepeis, N.E., Gabel, E.B., Ott, W.R., Switzer, P., 2009. Outdoor air pollution in
603 close proximity to a continuous point source. *Atmospheric Environment*, 43,
604 3155-3167.
605
606 Klepeis, N.E., Ott, W.R., Switzer, P., 2007. Real-time measurement of outdoor
607 tobacco smoke particles. *Journal of the Air & Waste Management*
608 *Association*, 57, 522-534.
609
610 Li, L, Lee, E.S., Nguyen, C., Zhu, Y, 2020. Effect of propylene glycol,
611 vegetable glycerin, and nicotine on emissions and dynamics of electronic
612 cigarette aerosols. *Aerosol Science and Technology*, 54, 1270-1281.
613
614 Martuzevicius, D., Prasauskas, T., Setyan, A., O'Connell, G., Cahours, X.,
615 Julien, R., Colard, S., 2019. Characterization of the spatial and temporal
616 dispersion differences between exhaled e-cigarette mist and cigarette
617 smoke. *Nicotine & Tobacco Research*, 21, 1371-1377.
618

619 McBride, S.J., Ferro, A., Ott, W.R., Switzer, P., Hildemann, L.M., 1999.
620 Investigations of the proximity effect for pollutants in the indoor
621 environment. *Journal of Exposure Analysis and Environmental Epidemiology*,
622 9, 602-621.
623

624 Nguyen, C. Li, L., Sen, C. A., Ronquillo, E., Zhu, Y., 2019. Fine and ultrafine
625 particles concentrations in vape shops. *Atmospheric Environment*, 211, 159-
626 169.
627

628 Ott, W., Mathematical modeling of indoor air quality. In: *Exposure Analysis*.
629 Ott, W., Steinemann, A., Wallace, L. Eds.; Taylor & Francis Group: Boca
630 Raton, FL, 2007.
631

632 Ott, W.R., Acevedo-Bolton, V., Cheng, K.C., Jiang, R.T., Klepeis, N.E.,
633 Hildemann, L.M., 2014. Outdoor fine and ultrafine particle measurements at
634 six bus stops with smoking on two California arterial highways -- Results of a
635 pilot study. *Journal of the Air and Waste Management Association*, 64, 47-60.
636

637 Ott, W.R., Zhao, T., Cheng, K.C., Wallace, L.A., Hildemann, L.M., 2020.
638 Measuring indoor fine particle concentrations, emission rates, and decay
639 rates from cannabis use in a residence (submitted to *Atmospheric*
640 *Environment: X*).
641

642 Posis, A., Bellettiere, J., Liles, S., Alcaraz, J., Nguyen, B., Berardi, V., Klepeis,
643 N.E., Hughes, S.C., Wu, T., Hovell, M.F., 2019. Indoor cannabis smoke and
644 children's health. *Preventive Medicine Reports*, 14, 100853.
645 <https://doi.org/10.1016/j.pmedr.2019.100853> Accessed on January 24,
646 2021.

647

648 Thatcher, T.L., Lai, A.C.K., Moreno-Jackson, R., Sextro, R.G., Nazaroff, W.W.,
649 2002. Effects of room furnishings and air speed on particle deposition rates
650 indoors. *Atmospheric Environment*, 36, 1811-1819.

651

652 Wallace, L.A., Ott, W.R., Cheng, K.C., Zhao, T., Hildemann, L.M., 2021.
653 Method for estimating the volatility of aerosols using the Piezobalance:
654 Examples from vaping e-cigarette and marijuana liquids. *Atmospheric*
655 *Environment*, 253, 118379. <https://doi.org/10.1016/j.atmosenv.2021.118379>

656

657 Xiao, Y., Lv, Y., Zhou, Y., Liu, H., Liu, J., 2020. Size-resolved surface
658 deposition and coagulation of indoor particles. *International Journal of*
659 *Environmental Health Research*, 30, 251-267.

660

661 Zhao, T., Shu, S., Guo, Q., Zhu, Y., 2016. Effects of design parameters and
662 puff topography on heating coil temperature and mainstream aerosols in
663 electronic cigarettes. *Atmospheric Environment*, 134, 61-69.

664

665 Zhao, T., Nguyen, C., Lin, C.H., Middlekauff, H.R., Peters, K., Moheimani, R.,
666 Guo, Q, Zhu, Y., 2017. Characteristics of secondhand electronic cigarette
667 aerosols from active human use. *Aerosol Science and Technology*, 51, 1368-
668 1376.
669
670 Zhao, T., Cheng, K.C., Ott, W.R., Wallace, L., Hildemann, L.M., 2020.
671 Characteristics of secondhand cannabis smoke from common smoking
672 methods: calibration factor, emission rate, and particle removal rate.
673 *Atmospheric Environment* <https://doi.org/10.1016/j.atmosenv.2020.117731>
674 Accessed on January 24, 2021.

675

676 **Table 1.** Comparison of average exhalation peak velocity, average
677 exhalation duration, and decay rate between marijuana smoking versus
678 vaping for base-case indoor experiments (all the windows/doors closed
679 without fan operating).

680

	Average exhalation peak velocity^a (m/s)	Average exhalation duration^b (s)	Decay Rate (1/h)
Smoking	<i>n</i> = 8	<i>n</i> = 8	<i>n</i> = 8
Mean	0.99 (0.61)	2.30 (0.35)	0.46
(IQR) ^c			(0.19)
Vaping	<i>n</i> = 8 ^d	<i>n</i> = 8 ^d	<i>n</i> = 9
Mean	0.53 (0.34)	3.43 (1.00)	0.75
(IQR) ^c			(0.55)

681 ^a Exhalation peak velocity averaged over 5 puffs in each experiment

682 ^b Exhalation duration averaged over 5 puffs in each experiment

683 ^c Interquartile range (difference between 75th and 25th percentiles)

684 ^d Did not take the measurement in 1 of the 9 vaping experiments

685

686

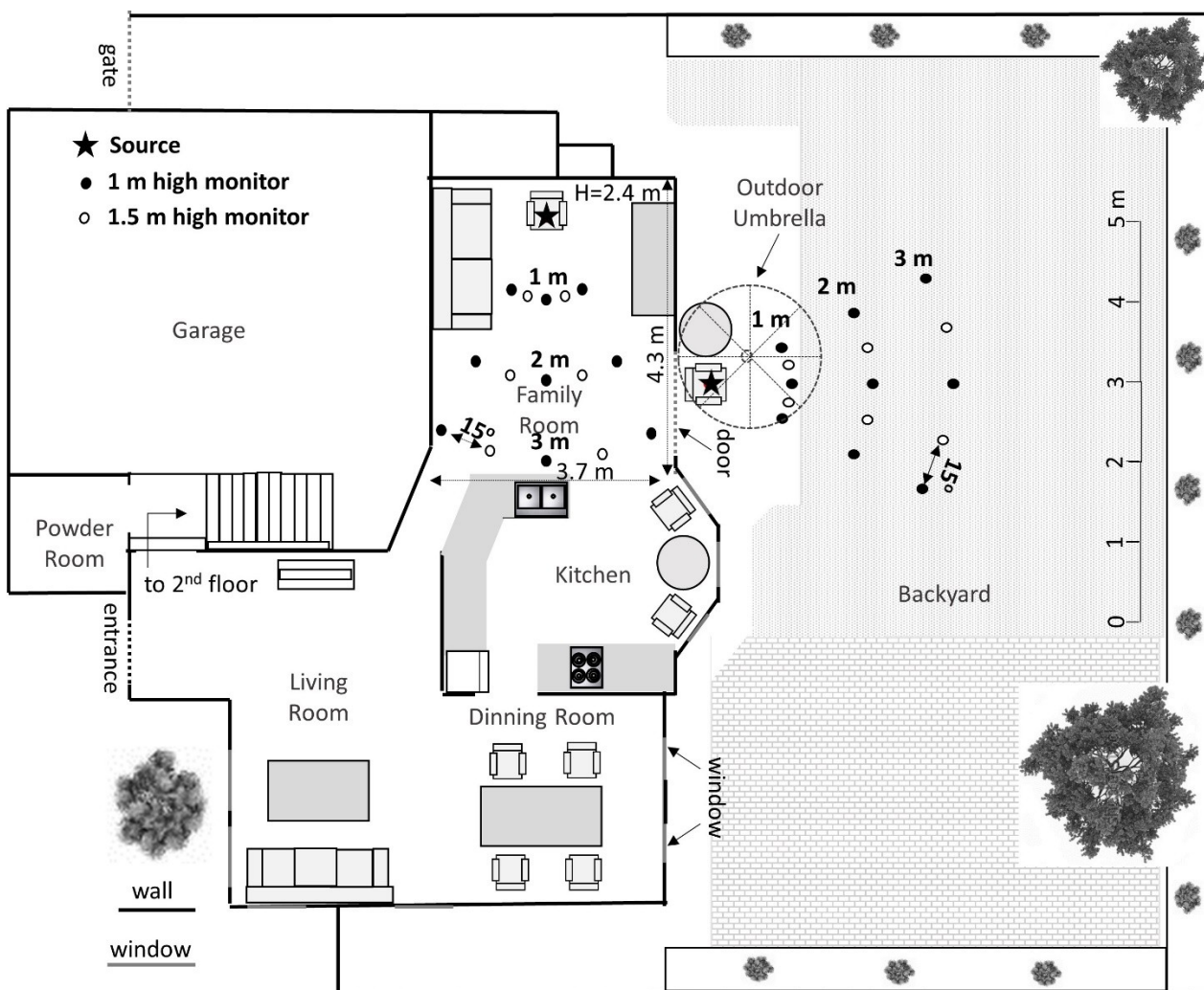
687 **Figure 1.** Indoor and outdoor monitoring setups in participant's house.

688 SidePak monitors (black and white circles) were facing the front of the

689 smoker (star) sitting either on the chair in the family room or the chair in the

690 backyard under the outdoor umbrella.

691



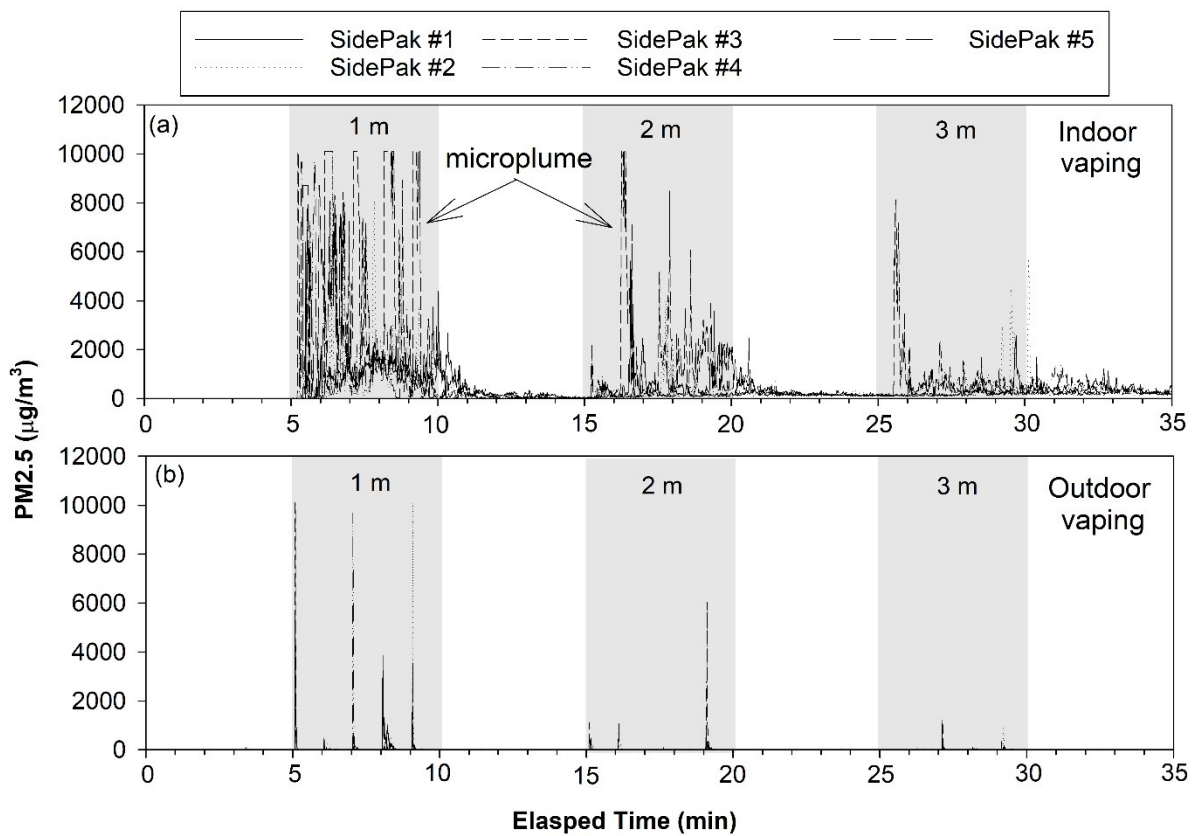
692

693

694

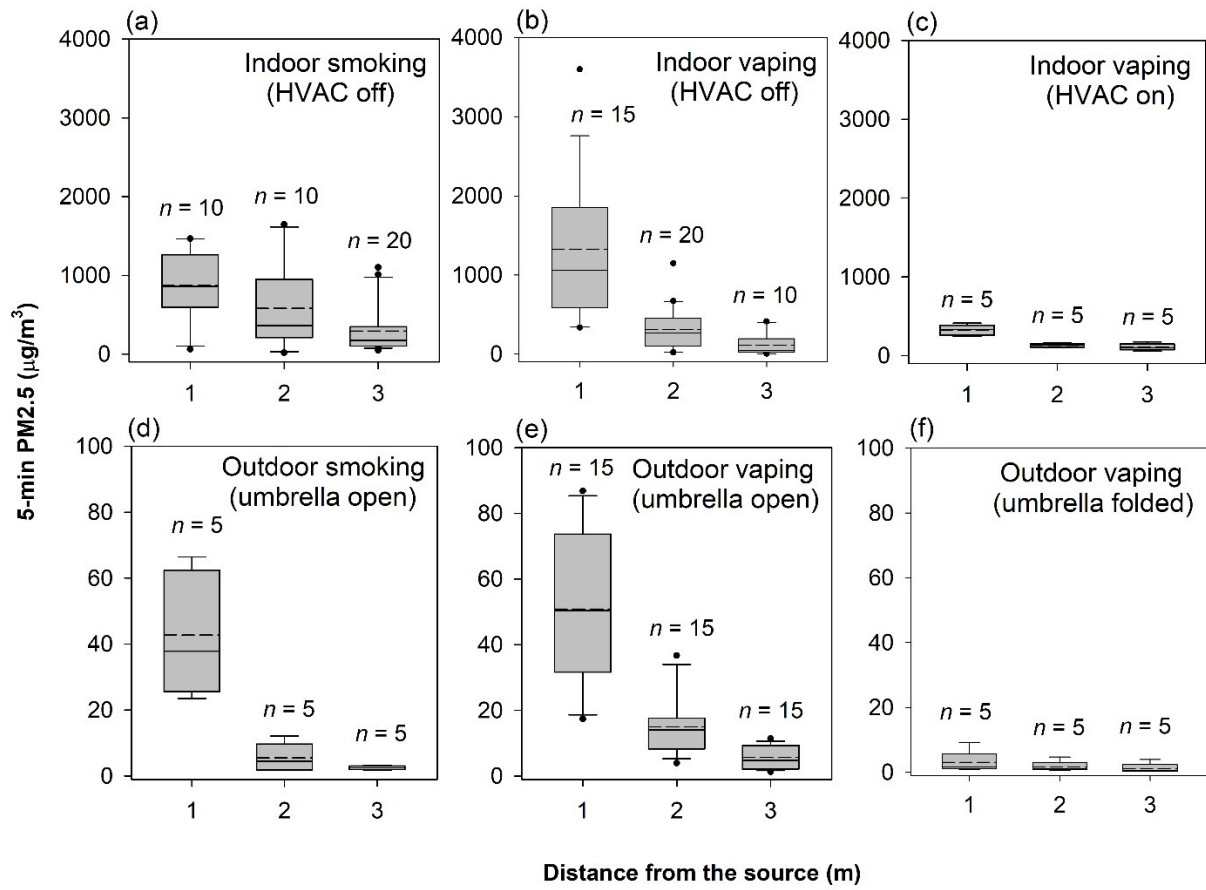
695

696 **Figure 2.** Example time series of 1-s $PM_{2.5}$ concentrations measured (a)
 697 indoors and (b) outdoors by 5 SidePak monitors (#1, #2, #3, #4, #5) at 1, 2,
 698 and 3 m distances from marijuana vaping. In each time series, monitors were
 699 moved between different distances between successive source periods (grey
 700 areas).



701
 702
 703
 704
 705
 706

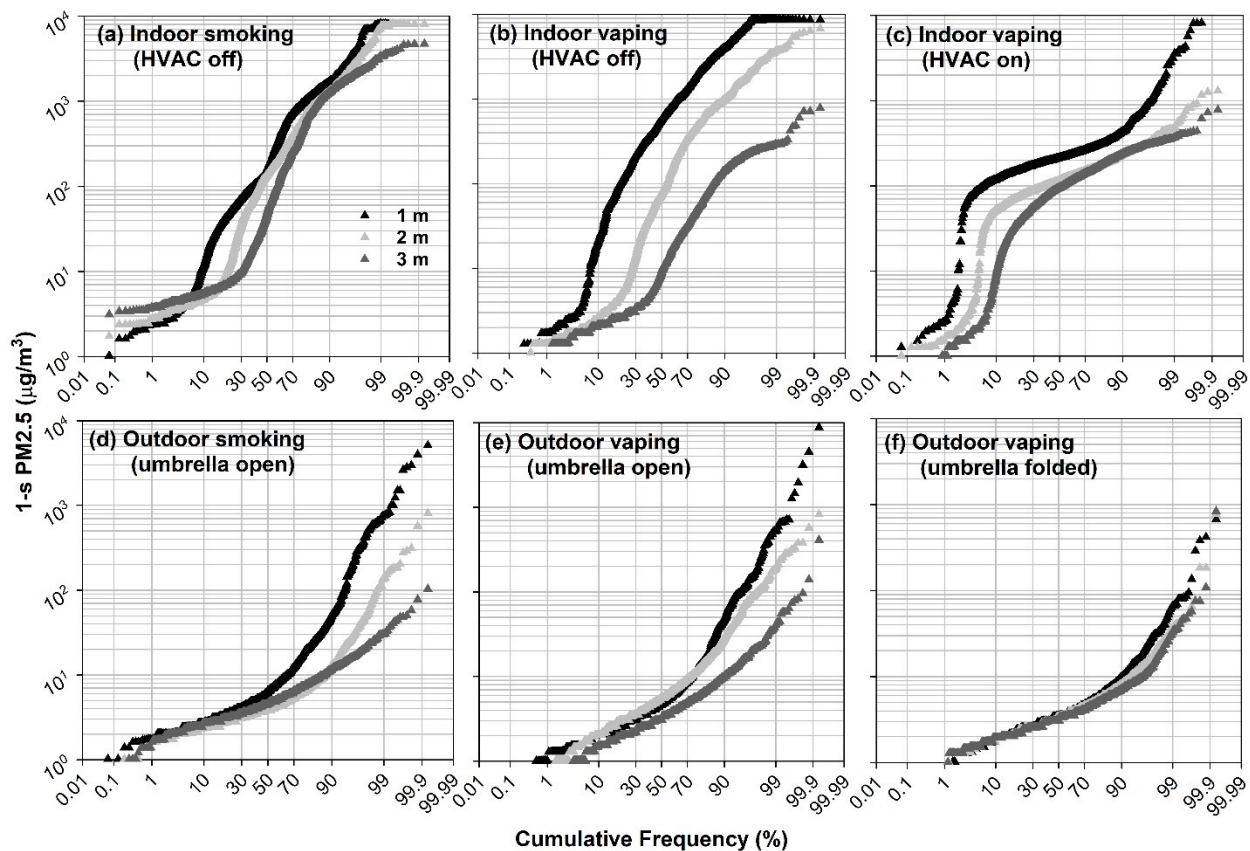
707 **Figure 3.** 5-min PM_{2.5} exposures at 1, 2, and 3 m distances from the source
708 for (a) indoor smoking with all windows and doors closed and HVAC off (base
709 case), (b) indoor vaping with all windows and doors closed and HVAC off
710 (base case), (c) indoor vaping with the HVAC fan operating and 1 door and 2
711 windows opened (alternative case), (d) outdoor smoking with the outdoor
712 umbrella above the smoker opened (base case), (e) outdoor vaping with the
713 outdoor umbrella above the smoker opened (base case), and (f) outdoor
714 vaping with the overhead outdoor umbrella folded (alternative case). The
715 boxes are the 25th and 75th percentiles; the whiskers are the 10th and 90th
716 percentiles; the dots are outliers. The dashed lines are the means and the
717 solid lines are the medians.



718

719

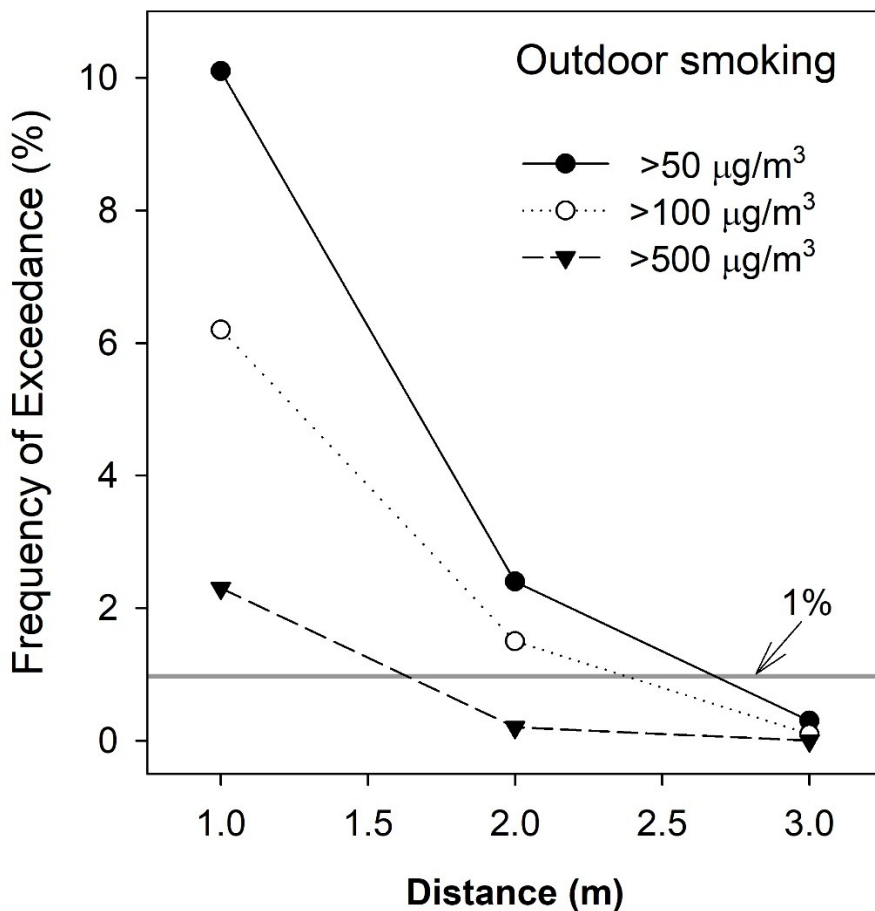
720 **Figure 4.** Cumulative frequency distributions of 1-s $PM_{2.5}$ concentrations at
 721 1, 2, 3 m distances from the source on log-probability graphs for (a) indoor
 722 smoking with all windows and doors closed and HVAC off (base case), (b)
 723 indoor vaping with all windows and doors closed and HVAC off (base case),
 724 (c) indoor vaping with the HVAC fan operating and 1 door and 2 windows
 725 opened (alternative case), (d) outdoor smoking with the outdoor umbrella
 726 above the smoker opened (base case), (e) outdoor vaping with the outdoor
 727 umbrella above the smoker opened (base case), and (f) outdoor vaping with
 728 the overhead outdoor umbrella folded (alternative case).



729

730

732 **Figure 5.** Example plot showing frequencies of exceeding 3 transient
733 exposure limits (50, 100, 500 $\mu\text{g}/\text{m}^3$) at 1, 2, and 3 m distances from the
734 source for outdoor smoking (based on data from Figure 4(d)).



735
736
737
738
739